Geochemical, biological and clumped isotopologue evidence for substantial microbial methane production under carbon limitation in serpentinites of the Samail ophiolite, Oman

Daniel B. Nothaft[a,*], Alexis S. Templeton[a,*], Jeemin H. Rhim[b], David T. Wang[b,1], Jabrane Labidi[c], Hannah M. Miller[a,2], Eric S. Boyd[d], Juerg M. Matter[e], Shuhei Ono[b], Edward D. Young[c], Sebastian H. Kopf[a], Peter B. Kelemen[f], Mark E. Conrad[g], The Oman Drilling Project Science Team

[a] *Department of Geological Sciences, University of Colorado, Boulder, CO, USA*
[b] *Department of Earth, Atmospheric and Planetary Sciences, Massachusetts Institute of Technology, Cambridge, Massachusetts, USA*
[c] *Department of Earth, Planetary, and Space Sciences, University of California, Los Angeles, CA, USA*
[d] *Department of Microbiology & Immunology, Montana State University, Bozeman, MT*
[e] *National Oceanography Centre, University of Southampton, Southampton, UK*
[f] *Lamont-Doherty Earth Observatory, Columbia University, Palisades, NY, USA*
[g] *Lawrence Berkeley National Laboratory, Berkeley, CA, USA*

Supplementary Materials

Contents

List of Figures

*Corresponding authors
Email addresses: daniel.nothaft@colorado.edu (Daniel B. Nothaft), alexis.templeton@colorado.edu (Alexis S. Templeton)
[1]Current address: ExxonMobil Upstream Research Company, Spring, TX 77389, USA
[2]Current address: Itasca Denver, Inc., 143 Union Blvd. Suite 525 Lakewood, CO 80228, USA

S1. Overview of CH_4 dynamics in other states of the system: wells WAB56, WAB71, and CM2A

Here, we briefly discuss three more wells to provide a broader perspective on CH_4 dynamics in the Samail ophiolite. The first of these wells is WAB56, which is situated in a catchment dominated by harzburgite (Main Text Figure 1; Figure S1; Main Text Table 1; also, WAB56 is pictured in Figure 1b of Rempfert et al. (2017)). Thus, the hydrogeologic setting of WAB56 is similar to that of NSHQ14. Yet, in comparison to fluids from NSHQ14, fluids sampled from WAB56 in 2015, 2016, and 2017 had lower pH, $c_{\sum \mathrm{Ca}}$, $c_{\mathrm{H_2}}$, $c_{\mathrm{CH_4}}$, and $\delta^{13}\mathrm{C}_{\mathrm{CH_4}}$ (Main Text Table 1, Main Text Table 3, Main Text Table 4; Rempfert et al., 2017). For example, fluids sampled from WAB56 in 2015 had a pH of 10.6, $c_{\sum \mathrm{Ca}}$ of $430\,\mu\mathrm{mol}\cdot\mathrm{L}^{-1}$, and $c_{\mathrm{H_2}}$ below quantitatable levels (Rempfert et al., 2017). Differences in fluid chemistry between WAB56 and NSHQ14 could be related to well construction. While NSHQ14 was drilled to 304 m depth and is cased only to 5.8 m, WAB56 was drilled to 106 m depth and is fully cased with a screened interval from 7 mbgl to 27 mbgl (Main Text Table 1). Thus, the fluids sampled from WAB56 may have derived from a shallow aquifer containing fluids of relatively short residence time, or a mixture of deep and shallow peridotite-reacted waters. Fluids sampled from WAB56 in 2015 had $\delta^{13}\mathrm{C}_{\mathrm{CH_4}}$ of $-83.2\,‰$ VPDB and 4 % of 16S rRNA gene reads of subsurface biomass affiliated with *Methanobacterium*, which is remarkably similar to fluids sampled from WAB188 in the same year ($\delta^{13}\mathrm{C}_{\mathrm{CH_4}}$ of $-71.3\,‰$ VPDB and 8 % of 16S rRNA gene reads of subsurface biomass assigned to *Methanobacterium*) (Main Text Table 4; Rempfert et al., 2017). Thus, it seems that the casing construction at WAB56 has restricted sampling to shallow waters of relatively low pH, $c_{\mathrm{Ca^{2+}}}$, and $c_{\mathrm{H_2}}$, where conditions of H_2 limitation and excess $\sum \mathrm{CO_2}$ allow the classic isotope effect of hydrogenotrophic methanogenesis to be expressed, as at WAB188.

Well WAB71 is located 2.4 km north of NSHQ04, and is set in dunite, 30 m east of a faulted contact with harzburgite (Main Text Figure 1; Figure S1; Main Text Table 1). It is similar to NSHQ04 in aqueous chemical composition ($\mathrm{Ca^{2+}} - \mathrm{OH^-}$ water; Main Text Table 2), dissolved gas composition (high $\mathrm{CH_4/H_2}$ and $\mathrm{C_1/(C_2 + C_3)}$ ratios; Main Text Figure 2, Main Text Table 3), $\delta^{13}\mathrm{C}_{\mathrm{CH_4}}$ (interannual mean of $+3.3\,‰$ VPDB, $s = 0.5\,‰$, $n = 4$; Main Text Figure 3a; Main Text Table 4), and CH_4-cycling microbial community composition. The dominant CH_4-cycling taxon at WAB71 appears to be *Methylococcus*, which accounted for 1 % of 16S rRNA gene reads of DNA extracted from subsurface biomass obtained in 2018 from WAB71 (Figure S3), which is consistent with prior sampling at this well (mean 2015 through 2018 of 1 %; Rempfert et al., 2017; Kraus et al., 2021). 16S rRNA gene reads affiliated with *Methanobacterium* were not detected at WAB71 in this study of samples obtained in 2018, but were found in low relative abundance ($< 1\,\%$ of reads) in samples from 2015 and 2017 (Rempfert et al., 2017; Kraus et al., 2021). The chemical and microbial similarities between WAB71 and NSHQ04 suggest that CH_4 cycle processes at WAB71 may be similar to those at NSHQ04, where a dominantly microbial source of CH_4 and an important role of aerobic

CH_4 oxidation were inferred. However, this conclusion is more speculative at WAB71, since it was not feasible to measure clumped isotopologue relative abundances in CH_4 from WAB71 by the methods of this study due to the relatively lower c_{CH_4} at WAB71 ($7.76\,\mu mol \cdot L^{-1}$ in 2018, $14.8\,\mu mol \cdot L^{-1}$ in 2017; Main Text Table 3). In addition, some aspects of WAB71 differ from NSHQ04. These include that WAB71 fluids have higher pH by 0.7 and lower δD_{CH_4} (interannual mean of -310 ‰ VSMOW, $s = 4$ ‰, $n = 2$; Main Text Figure 3a; Main Text Table 4). In addition, WAB71 had the lowest Eh (-229 mV; main text Table 1) and $c_{SO_4^{2-}}$ ($60.8\,\mu mol \cdot L^{-1}$) measured in groundwaters sampled in 2018. The reduced character and low $c_{SO_4^{2-}}$ of groundwaters sampled from WAB71 may be indicative of microbial SO_4^{2-} reduction at this well. Indeed, DNA extracted from subsurface samples from WAB71 had the highest 16S rRNA gene relative abundance of class Thermodesulfovibriona among wells sampled in 2018 (20 %; Figure S3; also mean of 19 % from 2015 to 2018; Rempfert et al., 2017; Kraus et al., 2021). Cultured representatives of Thermodesulfovibrionia are capable of SO_4^{2-} reduction coupled to H_2 oxidation and may additionally/alternatively oxidize C_1-C_3 acids and use thiosulfate, sulfite, Fe^{3+} or NO_3^- as terminal electron acceptors for anaerobic respiration (Henry et al., 1994; Sekiguchi et al., 2008). Further, 16S rRNA gene sequences affiliated with ANME-1b have been detected in DNA from WAB71, albeit in low relative gene abundance (< 1 % of reads in 2018; Main Text Figure 5; the same is true of samples from 2017 and 2015, but ANME-1b was not detected in 2016; Rempfert et al., 2017; Kraus et al., 2021). These data suggest that SO_4^{2-}-reducing bacteria may have contributed to the low c_{H_2} at WAB71, which may have allowed SO_4^{2-}-driven CH_4 oxidation by ANME-1b to be energetically competitive at this well, whereas it is apparently not in other sampled wells. The lower δD_{CH_4} at WAB71 relative to NSHQ04 could be due to a combination of aerobic and anaerobic methanotrophy at WAB71, which may have different C and H isotope effects than aerobic methanotrophy alone.

Well CM2A was drilled in the crust-mantle transition zone of the ophiolite by the Oman Drilling Project in late 2017 (Main Text Figure 1; Figure S1). Drill cuttings from the rotary-drilled well, CM2A, and cores from the adjacent diamond-wireline drilled well, CM2B, contain mostly dunite, with occasional gabbro and harzburgite (Main Text Table 1). Of the 300 m of core retrieved from CM2B, chromitite was noted only in one 30 cm-thick layer at 115 m depth. The water level in CM2A was 13.4 m, so these deep chromitites should be water-saturated and therefore not catalytic for CO_2 reduction to CH_4. CM2A contains $Ca^{2+} - OH^-$ waters with pH and major ion chemistry similar to NSHQ14 (Main Text Table 1; Main Text Table 2). Fluids sampled from CM2A had a c_{CH_4} of $152\,\mu mol \cdot L^{-1}$, which is almost double that of NSHQ14, concentrations of $C_2 - C_4$ *n*-alkanes up to $4.11 \cdot 10^{-2}\,\mu mol \cdot L^{-1}$, which is similar to or somewhat lower than those of NSHQ14, and a c_{H_2} of $3.38\,\mu mol \cdot L^{-1}$, which is 50 times lower than NSHQ14, although still higher than all other wells sampled in 2018 (Main Text Figure 2; Main Text Table 3). In comparison to NSHQ14 and NSHQ04, CH_4 in fluids sampled from CM2A had lower $\delta^{13}C$ (inter-laboratory mean of -4.3 ‰ VPDB; Main Text Table 4; Main Text Figure 3a). CH_4 from CM2A had the highest δD of all studied wells (inter-laboratory mean of -198 ‰ VSMOW; Main Text Table 4; Main Text Figure 3a). Values of $\varepsilon_{methane/water}$, $\Delta^{13}CH_3D$,

and $\Delta^{12}CH_2D_2$ indicate that CH_4 from CM2A is not in isotopic equilibrium with water, nor intramolecular equilibrium (Main Text Figure 3b and d; Main Text Table 4). 16S rRNA gene sequences affiliated with *Methanobacterium* were detected in DNA extracted from biomass in waters pumped from CM2A at low relative abundances ($< 1\,\%$ of reads; Figure S3). No sequences affiliated with methanotrophs were detected in DNA extracted from CM2A fluids (Main Text Figure 5). CM2A and NSHQ14 fluids share several relevant characteristics including isotopic disequilibrium in CH_4, detection of *Methanobacterium*, similar concentrations of major ionic species, and apparent scarcity of potentially catalytic, water-unsaturated chromitites. These similarities suggest that CH_4 in CM2A, like NSHQ14, is dominantly a mixture of abiotic CH_4 being released from fluid inclusions and microbial CH_4.

S2. Figures

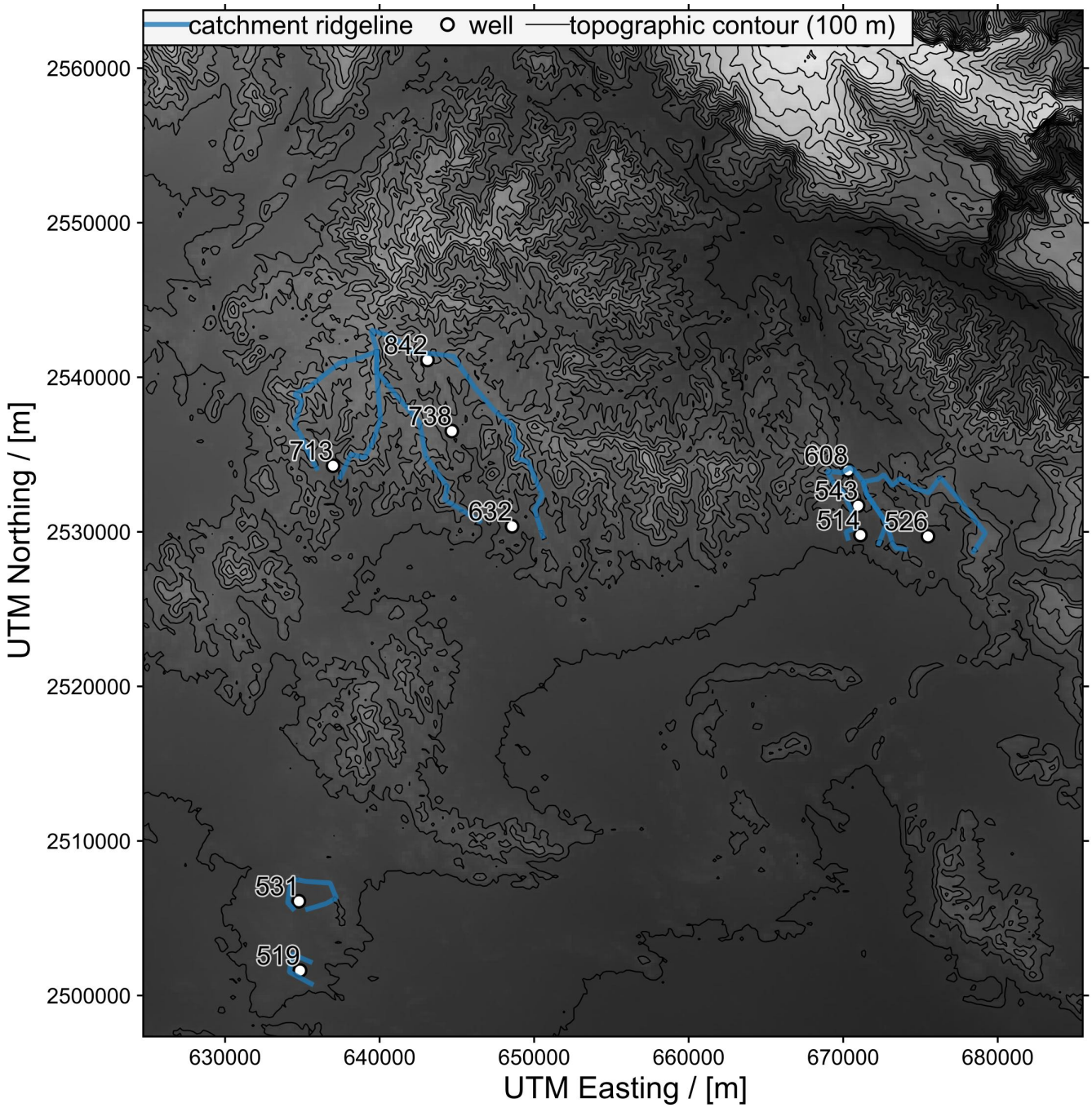

Figure S1: Study area in Samail ophiolite, Sultanate of Oman. Digital elevation model from USGS (2010). Elevations in meters above sea level are listed on the upper left of well location markers. Colors are scaled by elevation from low (dark) to high (light). Ridgelines of hydrologic catchments were estimated from the topography. If multiple wells shared catchment area, one catchment is depicted for visual clarity (i.e. WAB71, NSHQ04, and WAB188 share catchment area that is separate from NSHQ14; see Main Text Figure 1 for well names).

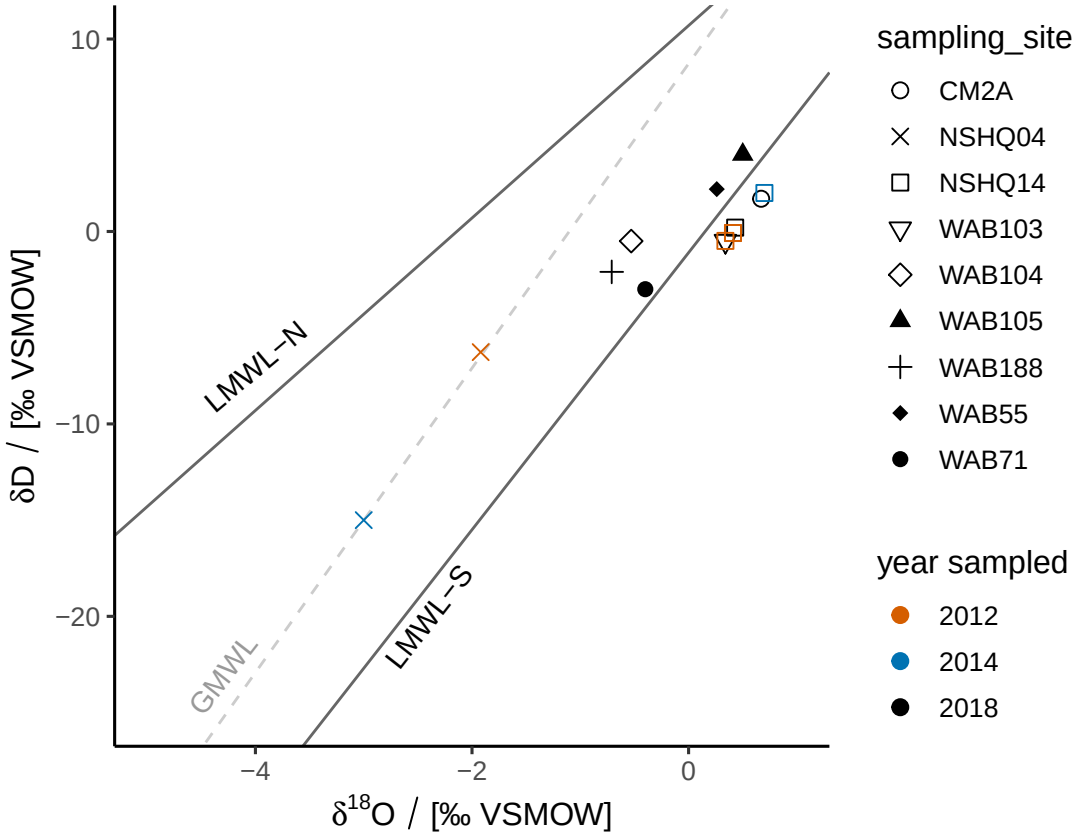

Figure S2: Plot of Oman groundwater stable isotopic compositions. Samples from 2012 were reported in Paukert Vankeuren et al. (2019). Samples from 2014 reported in Miller et al. (2016). *Abbreviations:* LMWL-N and LMWL-S, Oman local meteoric water lines derived from northern and southern sources, respectively (Weyhenmeyer et al., 2002); GMWL, global meteoric water line (Terzer et al., 2013).

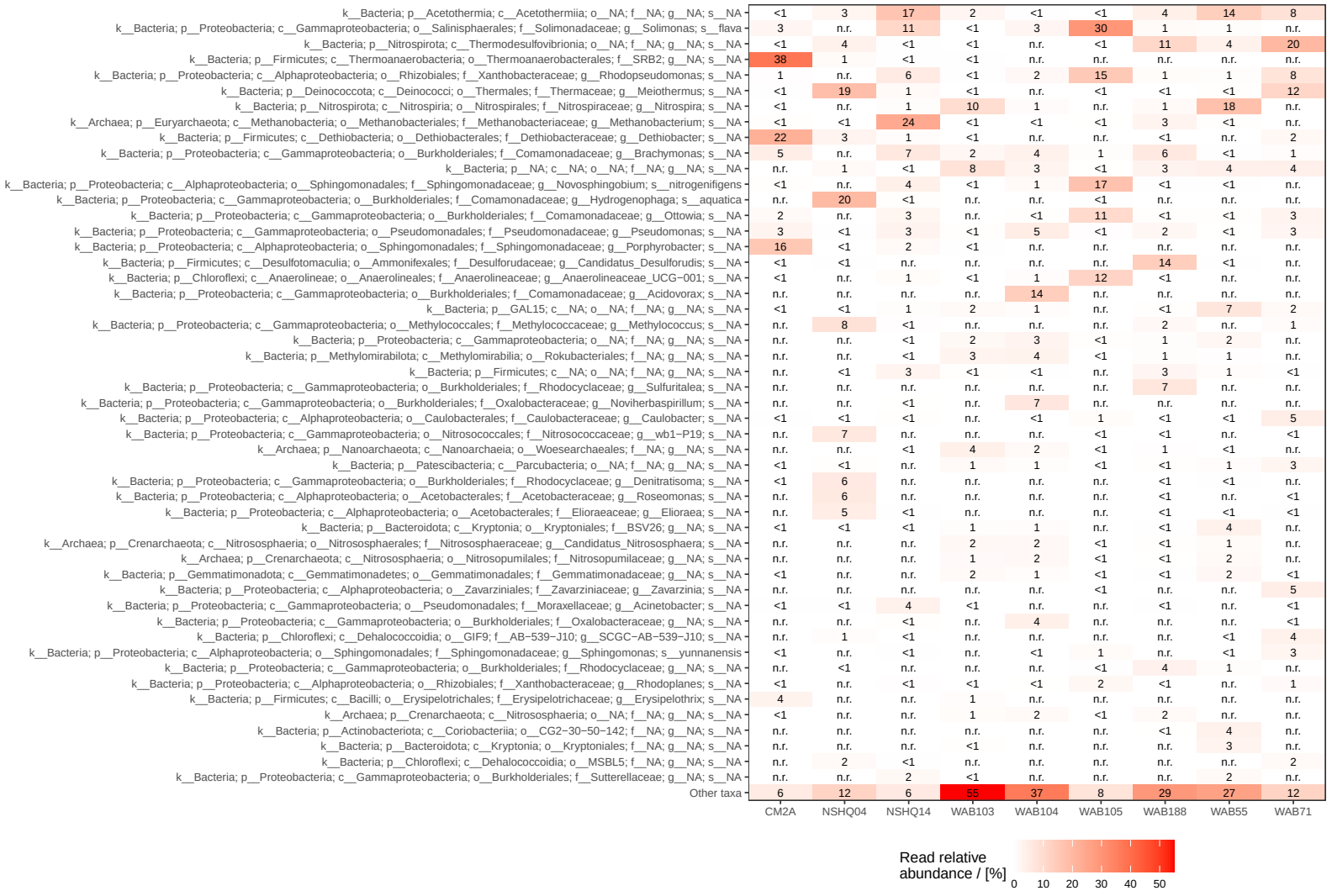

Figure S3: Heat map of the top 50 16S rRNA gene taxonomic assignments in samples obtained in 2018, arranged in descending order of abundance. Read relative abundances are reported as percentages rounded to the ones place. Cases when a taxon was detected in a sample and was $< 1\,\%$ read relative abundance after rounding are labeled "$<$ 1". Cases when no reads of a taxon were detected in a sample are labeled "n.r."

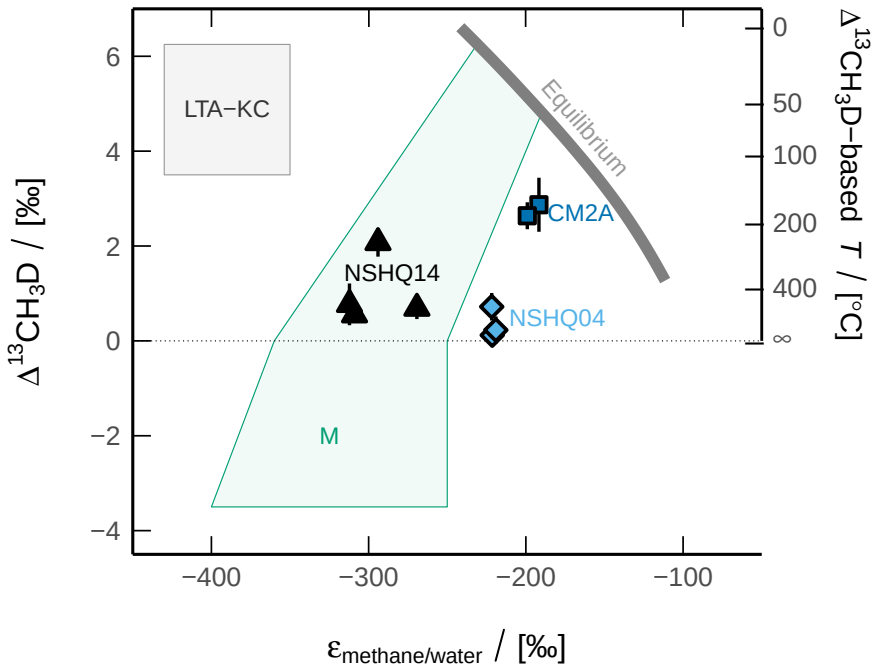

Figure S4: $\varepsilon_{methane/water}$ and $\Delta^{13}CH_3D$ plot of methane from Oman well waters, after Wang et al. (2015). Equilibrium (thick, light gray line) from Horibe and Craig (1995) and Young et al. (2017). *Abbreviations:* LTA-KC, low-temperature abiotic (Kidd Creek-type); M, microbial.

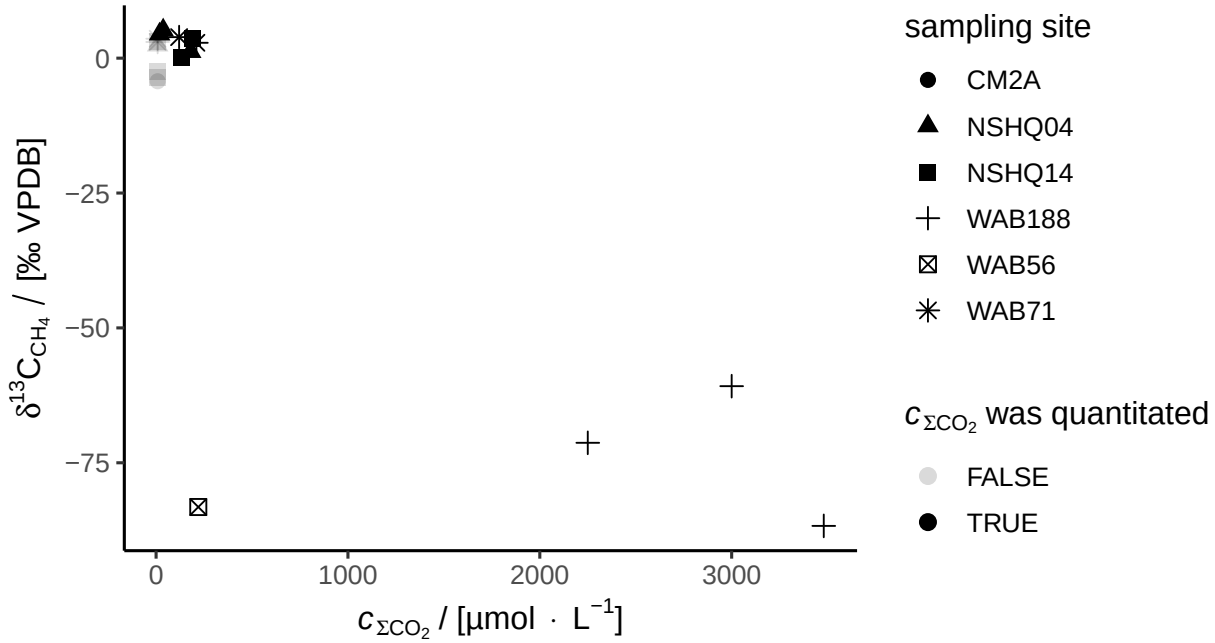

Figure S5: Plot of $c_{\sum CO_2}$ vs. $\delta^{13}C_{CH_4}$. Samples for which $c_{\sum CO_2}$ were not quantitated (which were all $Ca^{2+} - OH^-$ waters) are plotted at $8\,\mu mol \cdot L^{-1}$ and are colored in gray. This plot suggests an inverse relationship between $c_{\sum CO_2}$ and $\delta^{13}C_{CH_4}$, which is consistent with an effect of CO_2 availability on α_{CO_2/CH_4} of microbial methanogenesis. The data point from well WAB56 does not clearly conform to the proposed relationship. However, the well construction at WAB56 differs from the others, which may create conditions of H_2-limited hydrogenotrophic methanogenesis at WAB56, which could account for its relative low $\delta^{13}C_{CH_4}$ (Section S1).

S3. References

Henry, E.A., Devereux, R., Maki, J.S., Gilmour, C.C., Woese, C.R., Mandelco, L., Schauder, R., Remsen, C.C., Mitchell, R.. Characterization of a new thermophilic sulfate-reducing bacterium. Arch Microbiol 1994;161(1):62–69. URL: https://doi.org/10.1007/BF00248894. doi:10.1007/BF00248894.

Horibe, Y., Craig, H.. DH fractionation in the system methane-hydrogen-water. Geochim Cosmochim Acta 1995;59(24):5209–5217. doi:10.1016/0016-7037(95)00391-6.

Kraus, E.A., Nothaft, D., Stamps, B.W., Rempfert, K.R., Ellison, E.T., Matter, J.M., Templeton, A.S., Boyd, E.S., Spear, J.R.. Molecular Evidence for an Active Microbial Methane Cycle in Subsurface Serpentinite-Hosted Groundwaters in the Samail Ophiolite, Oman. Appl Environ Microbiol 2021;87(2). URL: https://aem.asm.org/content/87/2/e02068-20. doi:10.1128/AEM.02068-20. arXiv:https://aem.asm.org/content/87/2/e02068-20.full.pdf.

Miller, H.M., Matter, J.M., Kelemen, P., Ellison, E.T., Conrad, M.E., Fierer, N., Ruchala, T., Tominaga, M., Templeton, A.S.. Modern water/rock reactions in Oman hyperalkaline peridotite aquifers and implications for microbial habitability. Geochim Cosmochim Acta 2016;179:217 – 241. URL: http://www.sciencedirect.com/science/article/pii/S0016703716300205. doi:10.1016/j.gca.2016.01.033.

Paukert Vankeuren, A.N., Matter, J.M., Stute, M., Kelemen, P.B.. Multitracer determination of apparent groundwater ages in peridotite aquifers within the Samail ophiolite, Sultanate of Oman. Earth Planet Sci Lett 2019;516:37–48. doi:10.1016/j.epsl.2019.03.007.

123 Rempfert, K.R., Miller, H.M., Bompard, N., Nothaft, D., Matter, J.M., Kelemen, P., Fierer, N., Templeton, A.S.. Geological and geochemical controls on subsurface microbial life in the Samail Ophiolite, Oman. Front Microb 2017;8(56):1–21. doi:10.3389/fmicb.2017.00056.

126 Sekiguchi, Y., Muramatsu, M., Imachi, H., Narihiro, T., Ohashi, A., Harada, H., Hanada, S., Kamagata, Y.. Thermodesulfovibrio aggregans sp. nov. and Thermodesulfovibrio thiophilus sp. nov., anaerobic, thermophilic, sulfate-reducing bacteria isolated from thermophilic methanogenic sludge, and emended description of the genus Thermodesulfovibrio. Int J Syst Evol Microbiol 2008;58(11):2541–2548. URL: https://www.microbiologyresearch.org/content/journal/ijsem/10.1099/ijs.0.2008/000893-0. doi:10.1099/ijs.0.2008/000893-0.

131 Terzer, S., Wassenaar, L.I., Araguás-Araguás, L.J., Aggarwal, P.K.. Global isoscapes for δ^{18}O and δ^{2}H in precipitation: improved prediction using regionalized climatic regression models. Hydrol Earth Syst Sci 2013;17(11):4713–4728. URL: https://www.hydrol-earth-syst-sci.net/17/4713/2013/. doi:10.5194/hess-17-4713-2013.

134 USGS, . Digital Elevation - Global Multi-resolution Terrain Elevation Data 2010 (GMTED2010). 2010. doi:/10.5066/F7J38R2N.

135 Wang, D.T., Gruen, D.S., Lollar, B.S., Hinrichs, K.U., Stewart, L.C., Holden, J.F., Hristov, A.N., Pohlman, J.W., Morrill, P.L., Könneke, M., et al. Nonequilibrium clumped isotope signals in microbial methane. Science 2015;348(6233):428–431. doi:10.1126/science.aaa4326.

138 Weyhenmeyer, C.E., Burns, S.J., Waber, H.N., Macumber, P.G., Matter, A.. Isotope study of moisture sources, recharge areas, and groundwater flow paths within the eastern Batinah coastal plain, Sultanate of Oman. Water Resources Research 2002;38(10). doi:10.1029/2000WR000149.

141 Young, E., Kohl, I., Lollar, B.S., Etiope, G., Rumble Iii, D., Li, S., Haghnegahdar, M., Schauble, E., McCain, K., Foustoukos, D., et al. The relative abundances of resolved $^{12}CH_2D_2$ and $^{13}CH_3D$ and mechanisms controlling isotopic bond ordering in abiotic and biotic methane gases. Geochim Cosmochim Acta 2017;203:235–264. doi:10.1016/j.gca.2016.12.041.